ISSN 2514-3247

MINI-REVIEW

An insight into aptamer–protein complexes

Anastasia A Novoseltseva[1,2,*], Elena G Zavyalova[1,2], Andrey V Golovin[2,3], Alexey M Kopylov[1,2]

[1]Department of Chemistry, Lomonosov Moscow State University, Moscow, Russia; [2]Apto-Pharm Ltd., Moscow, Russia; [3]Department of Bioengineering and Bioinformatics, Lomonosov Moscow State University, Moscow, Russia

***Correspondence to:** Anastasia Novoseltseva, Email: novoseltsevaaa@gmail.com, Tel: +749 59393149, Fax: +749 59393181

Received: 04 May 2018 | **Revised:** 12 July 2018 | **Accepted:** 23 August 2018 | **Published:** 00 August **2018**

ISSN 2514-3247

ABSTRACT

A total of forty-five X-ray structures of aptamer–protein complexes have been resolved so far. We analysed a large dataset using common aptamer parameters such as the type of nucleic acid, aptamer length and presence of chemical modifications, and the various parameters of complexes such as interface area, number of polar contacts and Gibbs free energy change. We did not find correlation between Gibbs free energy change, interface area, or number of polar contacts. The elements of the dataset with heterogeneous parameters were clustered, providing a possibility to reveal structure–affinity relationship, SAR. Complexes with DNA aptamers and RNA aptamers had the same characteristics. Presence of aptamer modifications within the interface decreased Gibbs free energy change. Furthermore, a correlation between Gibbs free energy change and the interface area of complexes with modified aptamers was found. We also attempted to compare SAR for aptamer–protein complexes with antibody–protein SARs.

KEYWORDS: X-ray three-dimensional structure, aptamer, aptamer–protein complex, polar contact, interface area, structure–affinity relationship, SAR

INTRODUCTION

Aptamer research is an actively developing area with a growing number of new aptamers being selected for different targets. Several recent reviews mainly discuss aptamer selection techniques (Pfeiffer et al, 2017; Zhuo et al, 2017), modifications that improve affinity and stability of the aptamers (Ni et al, 2017; Biondi and Benner, 2018), and with their practical implementations (Nimjee et al, 2017; Poolsup and Kim, 2017). However, an understanding of structural background of aptamer functioning is scarce. Several attempts to understand a role of specific modifications in stabilizing of aptamer-protein complex has been made; for example, an effect of hydrophobic substituents on the average Gibbs free energy change of binding ΔG_b (Rohloff et al, 2014), and on the shape complementarity with protein surfaces (Gelinas et al, 2016) has been demonstrated. A comprehensive analysis of aptamer–protein complexes is of a great value, as it could reveal correlations between structure and affinity (SAR). For example, Dolot et al (2018) showed a decrease in the dissociation constant from 34 nM to 0.39 nM with the application of aptamer-protein structural understanding.

There are some challenges in resolving and examination of structures of aptamer-protein complexes. While the structure of the short unbounded aptamer can be readily studied by NMR (Sakamoto, 2017), an aptamer–protein complex has to be crystallized and studied with X-ray crystallography. Furthermore, combination of both NMR and X-ray crystallography is useful where aptamers undergo conformational rearrangement during interaction with protein (Davlieva et al, 2014).

This mini-review is focused on a comparison of known aptamer–protein structures. Intermolecular interfaces were examined by several parameters, including interface area and the number of polar contacts. A correlation between these parameters and affinity was also evaluated, aiming to find general recipes to decrease dissociation constant of aptamer-protein complexes.

PARAMETERS OF APTAMER–PROTEIN COMPLEXES

To initiate our analysis, we used several parameters including the type of nucleic acid (RNA or DNA), the presence of modified nucleotides, the length of the aptamer, and the value of the apparent dissociation constant aK_D.

To calculate the interface area, we applied AREAIMOL software. There is no recommended standard approach to calculate the values for the aptamer–protein complexes. We tested different programs for computing solvent accessible areas: PyMol (Ribeiro et al, 2015), FreeSASA (Mitternacht, 2016), AREAIMOL (Winn et al, 2011). A large difference was found between results due to inadequate calculations of modified nucleic acids. For example, the interface areas calculated for the modified RNA aptamer anti-Fc (PDB 3AGV) were the following: 878Å (PyMol), 314Å (FreeSASA), 444Å (AREAIMOL), while the published values are 580Å (Nomura et al, 2010) and 477Å (Rohloff et al, 2014; Gelinas et al, 2016). In contrast with other programs, AREAIMOL computes the interface areas regardless the chemical nature of the substituents in modified aptamers. Therefore, this software was used in the further calculations (Table 1).

PyMol software was used to compute the number of polar contacts (hydrogen bonds and electrostatic interactions) (Table 1). In our approach the polar contacts were not divided into hydrogen bonds and electrostatic interactions, because it was not productive. Such an attempt to consider these characteristics separately was made by Rohloff et al (2014).

The Gibbs free energy change of the complex formation ΔG_b is one of the main characteristics of affinity. The values were calculated for the complexes with known apparent dissociation constants of the given temperature, using the following equation:

$$\Delta G_b = -R \times T \times ln(aK_B) = R \times T \times ln(aK_D).$$

THE DATASET OF APTAMER–PROTEIN COMPLEXES

A previous publication studied a dataset of 19 structures (Gelinas et al, 2016). Since then (by January 2018), this number has increased to forty-five structures in the Protein Data Bank (PDB); all structures were solved by X-ray crystallography with the resolution between the range of 1.8 – 4.5Å. We examined all of them in this mini-review.

There are several intersections in the dataset. All forty-five structures are formed by thirty-five individual aptamers targeted to twenty-one different proteins (Table 2). Several complexes have been resolved more than once showing slight variations; like thrombin binding aptamer TBA, chelating either sodium or potassium cation in a complex with thrombin (PDB ID 4DIH and 4DII, respectively) (Russo-Krauss et al, 2012). In most cases, the unit cell of the crystal contains the unique conformation of the complex.

The “Gln-tRNA var AGGU” ‘aptamer’ was removed from our analysis, as it was created by modifying tRNA (Bullock et al, 2000). It is rather distinct from regular aptamers as being a derivative of the natural RNA with specific and highly ordered structure, and needs a special consideration.
The parameters of the aptamer–protein complexes exhibit great variation. For example, the interface area varies from 410Å^2 (Padlan et al, 2014) to 2088Å^2 (Kettenberger et al, 2006) (Supplementary Table 2). To get a general view, the interface areas were plotted against the aptamer length (Figure 1A). There were no obvious trends in this plot, probably due to simultaneous consideration of heterogeneous dataset. Therefore, an attempt to rank aptamers was made by organizing them into groups by their nature.

CLUSTER ANALYSIS REVEALED NO DISCREPANCY BETWEEN COMPLEXES OF PROTEINS WITH DNA AND RNA APTAMERS

The cluster analysis needs organisation of the dataset into subgroups. Firstly, we compared unmodified DNA aptamers with unmodified RNA aptamers. Single-stranded RNAs could form a large variety of tertiary structures compared to single-stranded DNA due to the sugar conformation (Gelinas et al, 2016). Moreover, conformational rearrangement of RNA aptamer could occur during binding to their target proteins (Bjerregaard et al, 2016; Gelinas et al, 2016). However, does any principal difference exist in organization of protein complexes with either DNA or RNA aptamers?

The results of cluster analyses are shown in Figure 1. We did not find a substantial difference between unmodified DNA- and RNA-based complexes; the complexes were indistinguishable on the various plots: interface area versus aptamer length, number of polar contacts versus interface area, and ΔG_b versus interface area (Figures 1B, C and D, respectively). Thus, both DNA and RNA aptamers binds proteins in a similar manner.

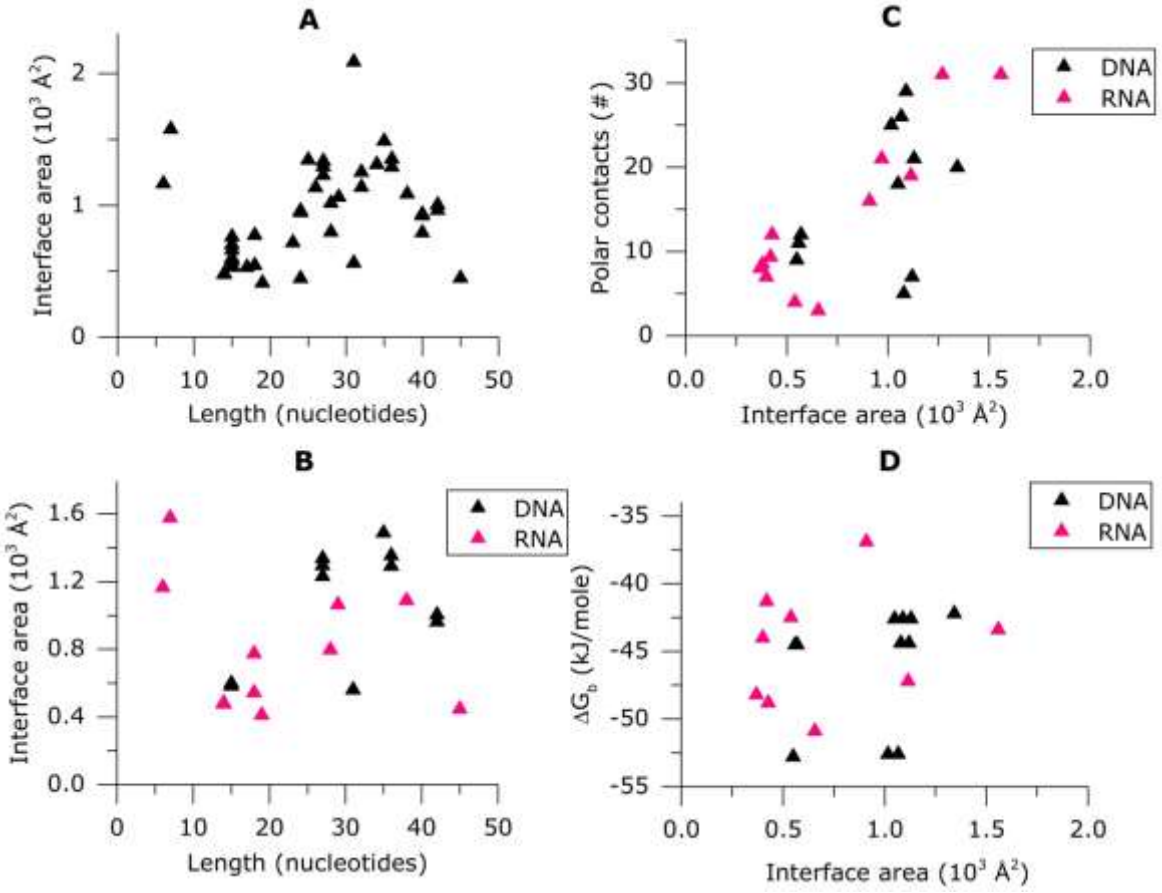

Figure 1. The cluster analysis of complexes of proteins with DNA and RNA aptamers. **A.** General analysis of complete dataset: interface area versus aptamer length, in nucleotides. **B-D.** Cluster analysis of unmodified DNA vs RNA aptamer complexes. Relationships between different structural parameters of complexes are shown: **B.** Interface area versus aptamer length. **C.** Number of polar contacts versus interface area. **D.** Gibbs free energy change versus interface area.

CLUSTER ANALYSIS REVEALED SIMILARITY IN ORGANISATION OF COMPLEXES WITH MODIFIED AND UNMODIFIED APTAMERS

If the nature of nucleic acid does not define the parameters of structure of aptamer–protein complexes, what about chemically modified nucleic acids? Introducing different modifications into an aptamer is a widespread approach to improve affinity of the aptamers (Ni et al, 2017). Is it really effective? A particular success story has been reported for aptamers with hydrophobic modifications (Slow Off-rate Modified Aptamers, "SOMAmers"). These modifications decrease dissociation rates of aptamer-protein complexes (Gelinas et al, 2016). We thus extended the dataset with various chemical modification types in the cluster analysis.

Aptamers were divided into three groups. The first and the largest group included unmodified aptamers and aptamers with modifications in non-interface regions. For example, aptamer ARC1172 for von Willebrand factor (Huang et al, 2009) contains a 3'-terminal inverted T. This link was introduced to increase exonuclease stability (Kratschmer and Levy, 2017), and has no effect on the functional activity of the aptamer. The second group included aptamers with modified bases. For example, there are aptamers with hydrophobic substituents in the 5-position of deoxyuridine, such as indole (T4W aptamer), phenyl and naphtyl derivatives (SL4, SL5, SL1025, SL1049, and SL1067 aptamers) and abasic sites (F5/2AP10), among others. The third group included aptamers with modifications of sugar-phosphate backbone, like 2'-substituted nucleotides, DNA with 5'-5' inversion between nucleotides, and L-configuration of pentose. Cluster analysis revealed that complexes with modified aptamers and with unmodified ones have no significant differences on the plots of interface areas versus length of aptamer (Figure 2A), and number of polar contacts versus interface areas (Figure 2B).

Next we considered the effect of modifications on the aptamer affinity. Aptamers can be split into two groups based on the arbitrary border at ΔG_b = -50kJ/mol (Figure 2C). The majority of the complexes with ΔG_b value below -50kJ/mol contain aptamers with modifications (14 out of 18), whereas only one-quarter of aptamers with ΔG_b value above this threshold is modified (7 out of 27). This distribution supports the usefulness of modifying aptamers as an approach to improve the affinity. However, the dataset size thus far is not sufficient to distinguish between the effect of specific types of modifications, as just a few structures have been resolved for each type. Therefore,

further efforts in solving structures of aptamer complexes are required to provide more relevant and detailed analysis.

Overall, the cluster analysis revealed the similarity in properties of complexes with modified and unmodified aptamers. The main difference between these clusters is in ΔG_b; an effort to find correlation between ΔG_b and structure parameters is discussed in the section on structure-affinity relationship in the aptamer-protein complexes below.

INTERRELATION BETWEEN NUMBER OF POLAR CONTACTS AND INTERFACE AREA

Previously, it was proposed that the interface area and the number of polar contacts for aptamer–protein complexes are interrelated (Rohloff et al, 2014; Gelinas et al, 2016). Rohloff and colleagues analysed eleven structures of aptamer-protein complexes and SOMAmers to support this suggestion (Rohloff et al, 2014). Here, we applied our own approach to the same dataset and gain the same results, *i.e.*, the number of polar contacts linearly depend on the interface area with the same correlation coefficient R^2 of 0.94 (Figure 2D). The coincidence of similar findings from these two approaches is noteworthy.

We extended the dataset to contain all known aptamer–protein complexes, except SOMAmers, and acquired the correlation with $R^2 = 0.43$ (Figure 2E). It is obvious that SOMAmers correspond to the overall trend. Then all modified aptamers were included to the dataset, and the same correlation coefficient, $R^2 = 0.40$, was obtained (Figure 2B). Thus, a relationship between the number of polar contacts and the interface area appears to exist in all aptamers.

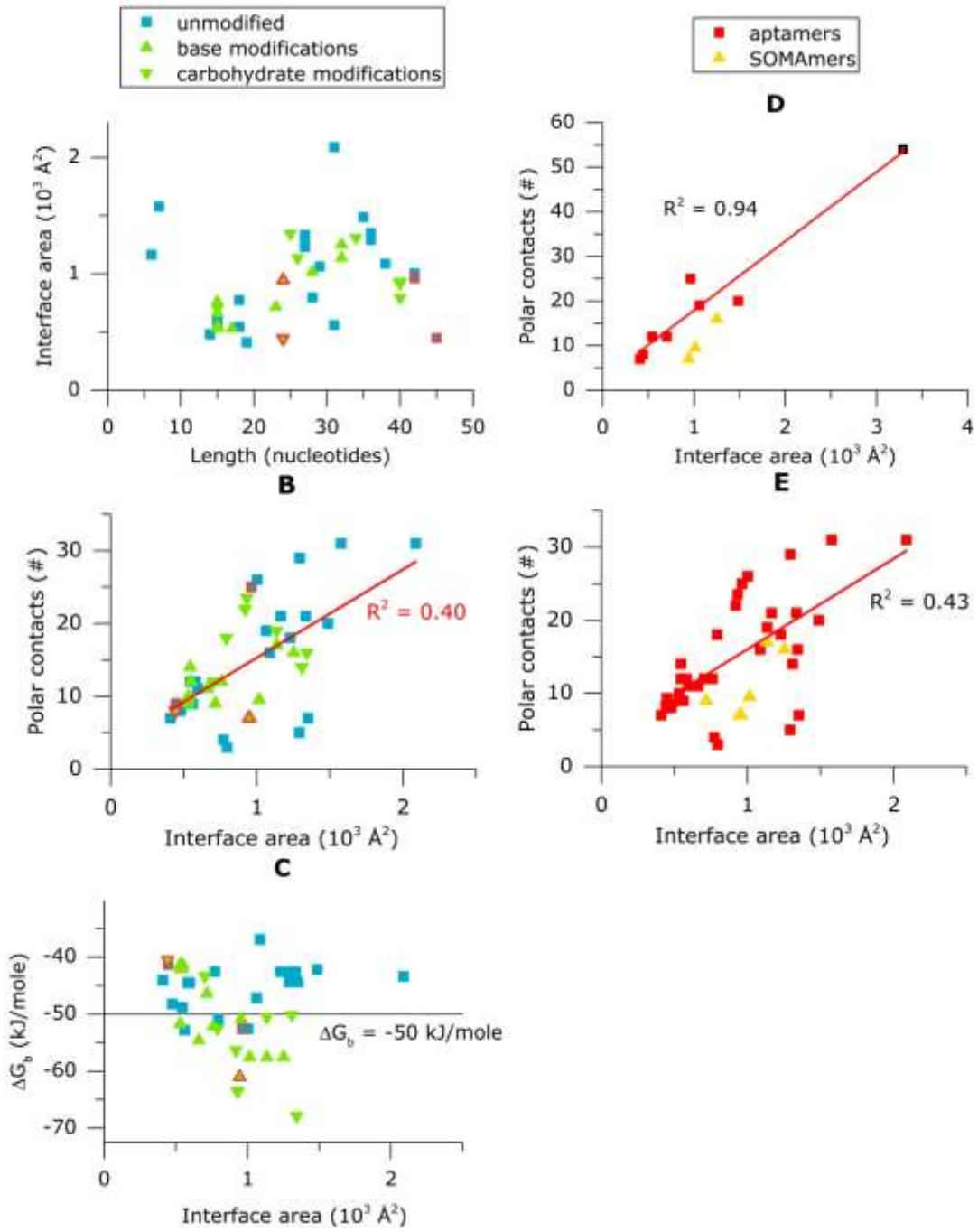

Figure 2. Comparison of modified and unmodified aptamer complexes. **A-C.** The cluster analysis of complexes of unmodified aptamers (in blue) versus modified ones (in green). The dots, outlined in red, correspond to the complexes chosen for detail head-to-head analysis (Figure 3). **A.** Interface area versus aptamer length in nucleotides. **B.** Number of polar contacts versus interface area, the linear approximation is shown for all aptamers. **C.** Gibbs free energy change versus interface area, the horizontal grid line is arbitrary border for ΔG_b. **D-E.** The correlation between polar contacts and interface area. **D.** Recalculated correlation for the dataset from Rohloff et al, 2014; the "Glu-tRNA var AGGU" dot, which significantly increase R^2, is outlined in black. **E.** Correlation for modern dataset from this mini-review.

HEAD-TO-HEAD COMPARISON ANALYSIS

In order to reveal the possible SARs, we chose pairs of aptamers, which were similar in one parameter but differed in another (Figures 2A, B, C). In addition, one aptamer has to belong to two pairs. MinF (Padlan et al, 2014) and anti-Fc (Nomura et al, 2010) had almost equal interface areas and number of polar contacts, but varied in length by almost twice (Figure 3A). SOMAmer SL5 (Davies et al, 2012) and aptamer anti-Fc have equal lengths and similar number of polar contacts, but interface areas differed twofold (Figure 3B). SL5 and ARC1172 (Huang et al, 2009) had equal interface areas, but substantially differed in length and number of polar contacts, in 1.8 and 3.6 times (Figure 3C). MinF and ARC1172 had similar length, but varied significantly in other parameters (Figure 3D). Furthermore, the chosen aptamers belonged to the different clusters, including unmodified RNA (MinF), unmodified DNA (ARC1172), DNA with base modifications (SL5), and RNA with modified sugar-phosphate backbone (anti-Fc). These particular examples were randomly chosen to highlight some common trends for aptamers with different characteristics.

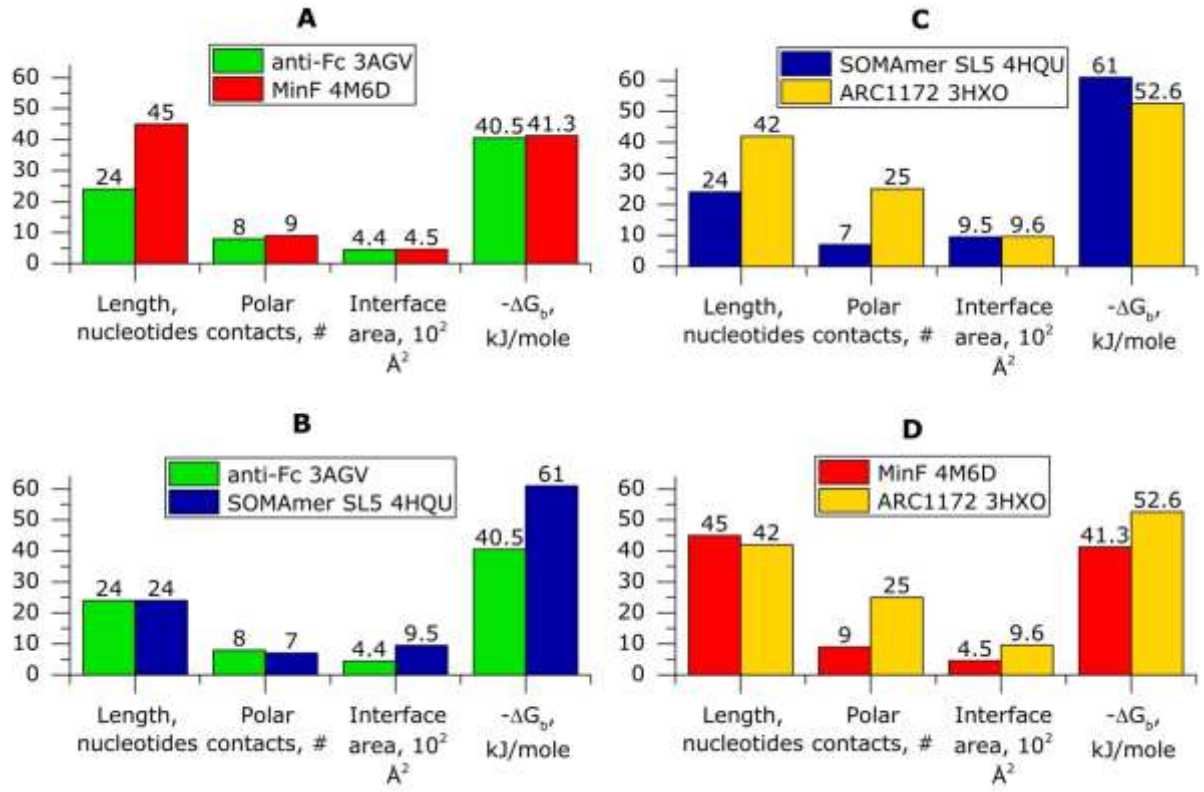

Figure 3. The pairwise head-to-head comparison of four chosen complexes. The following parameters were applied: aptamer length, number of polar contacts, interface area, Gibbs free energy change of binding.

The results of the analysis are intriguing (Figure 3). The first pair, MinF and anti-Fc (Figure 3A), has the same interface area, number of polar contacts, and absolute value of ΔG_b, although the lengths differ significantly. Thus in this particular case, the aptamer length does not determine affinity.

In the second example the difference between ΔG_b of SL5 and anti-Fc is as high as 20kJ/mole. This increase in absolute value of ΔG_b correlates with the two-fold increase in interface area (Figure 3B). In the pair SL5 and ARC1172 the numbers of polar contacts differ by 3.6 times, while the interface areas are equal. The $-\Delta G_b$ decreases by 8kJ/mole with the increase of the number of polar contacts (Figure 3C). We can assume that the number of polar contacts do not contribute crucially to affinity, when interface areas are rather large. Thus, in summary, the interface area plays a crucial role in the large absolute values of ΔG_b.

STRUCTURE-AFFINITY RELATIONSHIP IN THE APTAMER–PROTEIN COMPLEXES

As we found in comparing pairs of aptamers, the ΔG_b did not have an obvious correlation with the number of polar contacts, but it did with interface area. However, is this partial observation correct for all other aptamer complexes? As shown in Figure 4A-B, the ΔG_b values of known aptamer–protein complexes did not correlate with the number of polar contacts, and ΔG_b did not correlate with the interface area. The most informative example of pairwise comparison came from modified aptamers (Figure 3B). When we plotted ΔG_b versus number of polar contacts for complexes with modified aptamers only, a weak correlation can be found, $R^2 = 0.2$ (Figure 4D). On the contrary, the plot of ΔG_b versus the interface area showed a clear correlation, $R^2 = 0.53$ (Figure 4C).

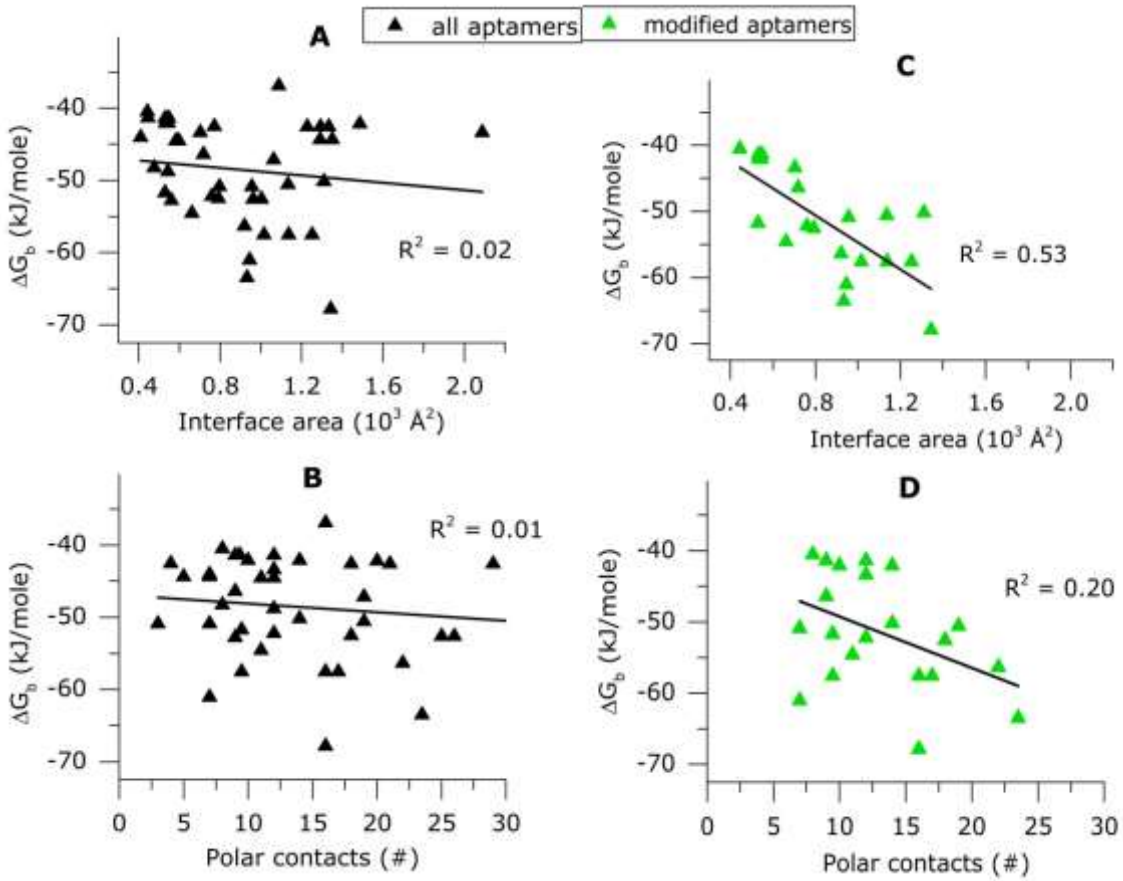

Figure 4. The searching for the SAR. Dependence of Gibbs free energy change on either interface area (**A**) or number of polar contacts (**B**) for all known aptamer–protein complexes. **C and D.** Dependence of Gibbs free energy change on either interface area or number of polar contacts, respectively, for complexes with modified aptamers.

Thus, in this analysis SAR was not revealed for unmodified aptamers, while it appears that for modified aptamers, the interface area plays crucial role. The results about SAR for unmodified aptamers could be understood from the known examples of SAR for other molecular recognition molecular, the antibodies. Several attempts have already been made to establish SAR for antibody–protein complexes. For example, the importance of the interface area for affinity has been previously illustrated by Chen et al (2013). The role of specific contacts for interacting proteins has also been demonstrated (Dalkas et al, 2014), *e.g.,* "hot-spot", a single contact, which is crucial for the total complex affinity (Jubb et al, 2012). The searching of hot spots can be productive in the case of aptamers. Analysis of aptamer–protein complexes is still in its infancy and is not at the same level as for the antibody complexes. Thus further detailed analysis using extended datasets could reveal additional structural parameters influencing affinity of the aptamers.

CONCLUSIONS

In this mini-review, we studied a dataset of forty-five aptamer–protein complexes with AREAIMOL program using parameters, such as types of nucleic acid, aptamer length and presence of chemical modifications, interface area, number of polar contacts as well as Gibbs free energy change of binding. These heterogeneous parameters of dataset were clustered, making it possible to reveal the structure–affinity relationship, SAR. For unmodified aptamers, we did not find a correlation between Gibbs free energy change and structure. The presence of aptamer modifications within the interface decreased Gibbs free energy change in proportion to the interface area. A range of modifications were analysed, but the number of resolved structures with particular type of modification is not yet enough for a detailed analysis. The nature of polar contacts is still beyond the scope of modern analysis, but the overall number of polar contacts did not correlate with the affinity. A detailed analysis of more extended datasets could reveal 'hot-spot' types of contacts that are found in antibody–protein complexes.

ACKNOWLEDGEMENTS

The research was supported by grants from the Russian Foundation for Basic Research (no. 17-00-00160 and 16-03-00136). The funders had no role in the study design, data collection and analysis, decision to publish, or preparation of the manuscript.

STATEMENT OF COMPETING INTERESTS

None declared.

LIST OF ABBREVIATIONS

aK_D: Apparent dissociation constant
NMR: Nuclear **M**agnetic **R**esonance
PDB: Protein **D**ata **B**ank
PDB ID: Identification code of the structure in Protein Data Bank
SAR: Structure-**A**ffinity **R**elationship
SOMAmer: Slow **o**ff-**R**ate **M**odified **A**pta**mer**

REFERENCES

Abeydeera ND, Egli M, Cox N, et al. 2016. Evoking picomolar binding in RNA by a single phosphorodithioate linkage. Nucleic Acids Res, 44, 8052-8064.

Biondi E, Benner SA. 2018. Artificially Expanded Genetic Information Systems for New Aptamer Technologies. Biomedicines, 6, 53-66.

Bjerregaard N, Andreasen PA, Dupont DM. 2016. Expected and unexpected features of protein-binding RNA aptamers. Wiley Interdiscip Rev RNA, 7, 744-757.

Bullock TL, Sherlin LD and Perona JJ. 2000. Tertiary core rearrangements in a tight binding transfer RNA aptamer. Nat Struct Biol, 7, 497-504.

Chen J, Sawyer N and Regan L. 2013. Protein-protein interactions: general trends in the relationship between binding affinity and interfacial buried surface area. Protein Sci, 22, 510-515.

Cheung YW, Kwok J, Law AW, Watt RM, Kotaka M and Tanner JA. 2013. Structural basis for discriminatory recognition of Plasmodium lactate dehydrogenase by a DNA aptamer. Proc Natl Acad Sci USA, 110, 15967-15972.

Dalkas GA, Teheux F, Kwasigroch JM and Rooman M. 2014. Cation-π, amino-π, π-π, and H-bond interactions stabilize antigen-antibody interfaces. Proteins, 82, 1734-1746.

Davies DR, Gelinas AD, Zhang C, et al. 2012. Unique motifs and hydrophobic interactions shape the binding of modified DNA ligands to protein targets. Proc Natl Acad Sci USA, 109, 19971-19976.

Davlieva M, Donarski J, Wang J, Shamoo Y and Nikonowicz EP. 2014. Structure analysis of free and bound states of an RNA aptamer against ribosomal protein S8 from Bacillus anthracis. Nucleic Acids Res, 42, 10795-10808.

Dolot R, Lam CH, Sierant M, et al. 2018. Crystal structures of thrombin in complex with chemically modified thrombin DNA aptamers reveal the origins of enhanced affinity. Nucleic Acids Res, 46, 4819-4830.

Gelinas AD, Davies DR, Edwards TE, et al. 2014. Crystal structure of interleukin-6 in complex with a modified nucleic acid ligand. J Biol Chem, 289, 8720-8734.

Gelinas AD, Davies DR and Janjic N. 2016. Embracing proteins: structural themes in aptamer-protein complexes. Curr Opin Struct Biol, 36, 122-132.

Hoehlig K, Maasch C, Shushakova N, et al. 2013. A novel C5a-neutralizing mirror-image (l-)aptamer prevents organ failure and improves survival in experimental sepsis. Mol Ther, 21, 2236-2246.

Huang DB, Vu D, Cassiday LA, Zimmerman JM, Maher LJ and Ghosh G. 2003. Crystal structure of NF-kappaB $(p50)_2$ complexed to a high-affinity RNA aptamer. Proc Natl Acad Sci USA, 100, 9268-9273.

Huang RH, Fremont DH, Diener JL, Schaub RG and Sadler JE. 2009. A structural explanation for the antithrombotic activity of ARC1172, a DNA aptamer that binds von Willebrand factor domain A1. Structure, 17, 1476-1484.

Jarvis TC, Davies DR, Hisaminato A, et al. 2015. Non-helical DNA Triplex Forms a Unique Aptamer Scaffold for High Affinity Recognition of Nerve Growth Factor. Structure, 23, 1293-1304.

Jubb H, Higueruelo AP, Winter A, Blundell TL. 2012. Structural biology and drug discovery for protein-protein interactions. Trends Pharmacol Sci, 33, 241-248.

Kato K, Ikeda H, Miyakawa S, et al. 2016. Structural basis for specific inhibition of Autotaxin by a DNA aptamer. Nat Struct Mol Biol, 23, 395-401.

Kettenberger H, Eisenfuhr A, Brueckner F, Theis M, Famulok M and Cramer P. 2006. Structure of an RNA polymerase II-RNA inhibitor complex elucidates transcription regulation by noncoding RNAs. Nat Struct Mol Biol, 13, 44-48.

Kratschmer C and Levy M. 2017. Effect of Chemical Modifications on Aptamer Stability in Serum. Nucleic Acid Ther, 27, 335-344.

Kretz CA, Stafford AR, Fredenburgh JC and Weitz JI. 2006. HD1, a thrombin-directed aptamer, binds exosite 1 on prothrombin with high affinity and inhibits its activation by prothrombinase. J Biol Chem, 281, 37477-37485.

Lee S, Song KM, Jeon W, Jo H, Shim YB and Ban C. 2012. A highly sensitive aptasensor towards Plasmodium lactate dehydrogenase for the diagnosis of malaria. Biosens Bioelectron, 35, 291-296.

Mitternacht S. 2016. FreeSASA: An open source C library for solvent accessible surface area calculations. F1000Res, 5, 189.

Miyakawa S, Nomura Y, Sakamoto T, et al. 2008. Structural and molecular basis for hyperspecificity of RNA aptamer to human immunoglobulin G. RNA, 14, 1154-1163.

Nagatoishi S and Sugimoto N. 2012. Interaction of water with the G-quadruplex loop contributes to the binding energy of G-quadruplex to protein. Mol BioSyst, 8, 2766-2770.

Nomura Y, Sugiyama S, Sakamoto T, et al. 2010. Conformational plasticity of RNA for target recognition as revealed by the 2.15 A crystal structure of a human IgG-aptamer complex. Nucleic Acids Res, 38, 7822-7829.

Ni S, Yao H, Wang L, et al. 2017. Chemical Modifications of Nucleic Acid Aptamers for Therapeutic Purposes. Int J Mol Sci, 18, 1683-1704.

Nimjee SM, White RR, Becker RC, Sullenger BA. 2017. Aptamers as Therapeutics. Annu Rev Pharmacol Toxicol, 57, 61-79.

Oberthur D, Achenbach J, Gabdulkhakov A, et al. 2015. Crystal structure of a mirror-image L-RNA aptamer (Spiegelmer) in complex with the natural L-protein target CCL2. Nat Commun, 6, 6923-6934.

Padlan CS, Malashkevich VN, Almo SC, Levy M, Brenowitz M and Girvin ME. 2014. An RNA aptamer possessing a novel monovalent cation-mediated fold inhibits lysozyme catalysis by inhibiting the binding of long natural substrates. RNA, 20, 447-461.

Pagano B, Martino L, Randazzo A and Giancola C. 2008. Stability and binding properties of a modified thrombin binding aptamer. Biophys J, 94, 562-569.

Parrott AM, Lago H, Adams CJ, Ashcroft AE, Stonehouse NJ and Stockley PG. 2000. RNA aptamers for the MS2 bacteriophage coat protein and the wild-type RNA operator have similar solution behavior. Nucleic Acids Res, 28, 489-497.

Pfeiffer F, Rosenthal M, Siegl J, Ewers J, Mayer G. 2017. Customised nucleic acid libraries for enhanced aptamer selection and performance. Curr Opin Biotechnol, 48, 111-118.

Poolsup S, Kim CY. 2017. Therapeutic applications of synthetic nucleic acid aptamers. Curr Opin Biotechnol, 48, 180-186.

Ren X, Gelinas AD, von Carlowitz I, Janjic N, Pyle AM. 2017. Structural basis for IL-1α recognition by a modified DNA aptamer that specifically inhibits IL-1α signaling. Nat Commun, 8, 810.

Ribeiro J, Melo F, Schüller A. 2015. PDIviz: analysis and visualization of protein-DNA binding interfaces. Bioinformatics. 2015, 31, 2751-2753.

Rohloff JC, Gelinas AD, Jarvis TC, et al. 2014. Nucleic acid ligands with protein-like side chains: modified aptamers and their use as diagnostic and therapeutic agents. Mol Ther Nucleic Acids, 3, e201.

Russo-Krauss I, Merlino A, Randazzo A, Novellino E, Mazzarella L and Sica F. 2012. High-resolution structures of two complexes between thrombin and thrombin-binding aptamer shed light on the role of cations in the aptamer inhibitory activity. Nucleic Acids Res, 40, 8119-8128.

Sakamoto T. 2017. NMR study of aptamers. Aptamers, 1, 13-18.

Someya T, Baba S, Fujimoto M, Kawai G, Kumasaka T and Nakamura K. 2012. Crystal structure of Hfq from Bacillus subtilis in complex with SELEX-derived RNA aptamer: insight into RNA-binding properties of bacterial Hfq. Nucleic Acids Res, 40, 1856-1867.

Spiridonova VA, Barinova KV, Glinkina KA, et al. 2015. A family of DNA aptamers with varied duplex region length that forms complexes with thrombin and prothrombin. FEBS Lett, 589, 2043-2049.

Tesmer VM, Lennarz S, Mayer G and Tesmer JJ. 2012. Molecular mechanism for inhibition of G protein-coupled receptor kinase 2 by a selective RNA aptamer. Structure, 20, 1300-1309.

Winn MD, Ballard CC, Cowtan KD, et al. 2011. Overview of the CCP4 suite and current developments. Acta Crystallogr D Biol Crystallogr, 67, 235-242.

Yatime L, Maasch C, Hoehlig K, Klussmann S, Andersen GR and Vater A. 2015. Structural basis for the targeting of complement anaphylatoxin C5a using a mixed L-RNA/L-DNA aptamer. Nat Commun, 6, 6481-6494.

Zhuo Z, Yu Y, Wang M, et al. 2017. Recent Advances in SELEX Technology and Aptamer Applications in Biomedicine. Int J Mol Sci, 18, 2142-2160.

Table 1. The structural and affinity characteristics of aptamer–protein complexes. IA – interface area, aK_D – apparent dissociation constant, ΔG_b – Gibbs free energy change during complex formation.

PDB ID	Length (nucleotides)	Polar contacts (number)	IA, Å^2	aK_D, nM	ΔG_b, kJ/mol
4PDB	38	16	1088	110 ± 30 (Davlieva et al, 2014)	-36.9
4WB3	40	22	921	0.035 (Yatime et al, 2015)	-56.3
4WB2		24	933	0.02 (Hoehlig et al, 2013)	-63.5
5HRT	34	14	1310	1.6 (Kato et al, 2016)	-50.2
4R8I	40	18	793	1.4 ± 0.2 (Oberthur et al, 2015)	-52.5
3AGV	24	8	444	75 (Miyakawa et al, 2008)	-40.5
1EXD	73	54	3290	0.3 ± 0.1 (Bullock et al, 2000)	-54.3
3UZS	28	3	797	1.2 ± 0.6 (Tesmer et al, 2012)	-50.9
3UZT	18	4	773	35 ± 5 (Tesmer et al, 2012)	-42.5
4NI7	32	17	1137	0.2 (Gelinas et al, 2014)	-57.6
4NI9		16	1253		
5UC6	23	9	718	7.3 (Ren et al, 2017)	-46.4
3ZH2	35	20	1487	51 ± 9 (Cheung et al, 2013)	-42.2
5HTO	36	5	1291	16.8 ± 0.6 (Lee et al, 2012)	-44.4
5HRU		7	1352		
4M6D	45	9	447	57 ± 3 (Padlan et al, 2014)	-41.3
4M4O	19	7	410	19 ± 2 (Padlan et al, 2014)	-44.0
5MSF	18	12	544	2.0 ± 0.4 (Parrott et al, 2000)	-48.8
7MSF	14	9	482	n.d.	n.d.
1U1Y	17	10	530	0.6 ± 0.3 (Parrott et al, 2000)	-51.7
6MSF	14	8	477	82 ± 6 (Parrott et al, 2000)	-48.2
4ZBN	28	10	1016	0.21 ± 0.08 (Jarvis et al, 2015)	-57.6
1OOA	29	19	1063	5 ± 2 (Huang et al, 2003)	-47.2
4HQX	24	7	957	1.2 (Davies et al, 2012)	-50.9
4HQU	24	7	946	0.02 (Davies et al, 2012)	-61.0
3HSB	7	31	1577	n.d.	n.d.
3AHU	6	21	1165	n.d.	n.d.
2B63	31	31	2088	33 ± 2 (Kettenberger et al, 2006)	-43.4
3DD2	26	19	1135	1.87 ± 0.04 (Abeydeera et al, 2016)	-50.6
5DO4	25	16	1344	0.0018 ± 0.0002 (Abeydeera et al, 2016)	-67.9
4I7Y	27	29	1294	29 ± 3 (Kretz et al., 2006)	-42.6
5EW1 /D		21	1135		
5EW2 /D		18	1229		
6EO6	15	11	760	1.00 (Dolot et al., 2018)	-52,2
6EO7	15	12	662	0.39 (Dolot et al., 2018)	-54,6
3QLP	15	12	703	25 ± 1 (Pagano et al, 2008)	-43.4
5CMX	31	9	561	0.56 (Spiridonova et al, 2015)	-52.8
4DII	15	12	583	34 ± 5 (Kretz et al., 2006)	-44.5
4DIH		11	597		
4LZ4	15	12	548	54.9 (Nagatoishi and Sugimoto, 2012)	-41.4
5EW1 /E		9	531		
4LZ1	15	14	545	39.1 (Nagatoishi and Sugimoto, 2012)	-42.1
5EW2 /E		10	533		
3HXQ	42	26	1003	0.66 ± 0.08 (Huang et al, 2009)	-52.6
3HXO		25	962		

Table 2. The known structures of aptamer–protein complexes. RNAa – RNA with 2-aminopurine nucleotide; DNAd – DNA with abased nucleotides; RNAf – RNA with 2'-fluorine nucleotide; DNAh – DNA with hydrophobic modifications; DNAi – DNA with inverted sugar-phosphate backbone; L-RNA, L-DNA – stereoisomeric nucleic acid form; DNAm – DNA with 2'-O-methyl modifications. C5a – C5a anaphylatoxin; CCL2 – C-C motif chemokine 2; ENPP 2 – Ectonucleotide pyrophosphatase/phosphodiesterase family member 2; GlnRS – Glutaminyl-tRNA synthetase; LD – Lactate dehydrogenase; NF-κB – Nuclear factor kappa-light-chain-enhancer of activated B cells; β-NGF - Nerve growth factor beta; PDGF-BB – Platelet-derived growth factor homodimer BB.

PDB ID	Reso-lution, Å	Target protein	Aptamer	Nucleic acid
4PDB	2.6	30S ribosomal protein S8 (*Bacillus anthracis*)	RNA-2	RNA
4WB3	2	C5a-desArg (*Mus musculus*)	NOX-D20	L-RNA/L-DNA
4WB2	1.8	C5a (*Mus musculus*)		
5HRT	1.997	ENPP 2 (*Mus musculus*)	RB011	DNAm
4R8I	2.05	CCL2 (*Homo sapiens*)	NOX-E36	RNA
3AGV	2.15	Fc region of IgG-1 (*Homo sapiens*)	anti-Fc	RNAf
1EXD	2.7	GlnRS (*Escherichia coli*)	Gln-tRNA var AGGU	RNA
3UZS	4.52	G-protein coupled receptor kinase 2 (*Bos taurus*)	C13.28	RNA
3UZT	3.51		C13.18	RNA
5UC6	2.1	Interleukin IL-1α (*Homo sapiens*)	SOMAmer SL1067	DNAh
4NI7	2.4	Interleukin IL-6 (*Homo sapiens*)	SOMAmer SL1025	DNAh
4NI9	2.55			
3ZH2	2.1	LD (*Plasmodium falciparum*)	2008s	DNA
5HTO	1.9	L-LD (*Plasmodium vivax*)	pL1	DNA
5HRU	1.7			
4M6D	2.68	Lysozyme C (Gallus gallus)	MinF (Padlan et al, 2014)	RNA
4M4O	2		MinE (Padlan et al, 2014)	RNA
5MSF	2.8	MS2 coat protein (*Escherichia phage*)	F5	RNA
7MSF	2.8		F7	RNA
1U1Y	2.8		F5/2AP10	RNAa
6MSF	2.8		F6	RNA
4ZBN	2.44	β-NGF (*Homo sapiens*)	SOMAmer SL1049	DNAh
1OOA	2.45	NF-κB (p50)2 (*Mus musculus*)	-	RNA
4HQX	2.3	PDGF-BB (*Homo sapiens*)	SOMAmer SL4	DNAh
4HQU	2.2		SOMAmer SL5	DNAh
3HSB	2.2	RNA-binding protein Hfq Sm-like (*Bacillus subtilis*)	Aptamers' consensus fragment (Someya et al, 2012)	RNA
3AHU	2.2			RNA
2B63	3.8	RNA polymerase II (*Saccharomyces cerevisiae*)	FC*	RNA
3DD2	1.9	Thrombin (*Homo sapiens*)	AF113-1	RNAf
5DO4	1.859		AF113-18	RNAf
4I7Y	2.4		HD22	DNA
5EW1	2.95			
5EW2	3.59			
6EO7	2.24		T4K (Dolot et al, 2018)	DNAh
6EO6	1.69		T4W (Dolot et al, 2018)	DNAh
3QLP	2.14		mTBA	DNAi
5CMX	2.98		RE31	DNA
4DII	2.05		TBA	DNA
4DIH	1.8			
4LZ4	2.56		TBAΔT3	DNAd
5EW1	2.95			
4LZ1	1.65		TBAΔT12	DNAd
5EW2	3.59			
3HXQ	2.694	Von Willebrand factor (*Homo sapiens*)	ARC1172	DNA
3HXO	2.4			

ISSN 2514-3247

1